

AUTOMATIC REGISTRATION SCHEMES APPLIED TO RETINAL IMAGES: AN EVALUATION STUDY

E. Karali*, P. Asvestas*, G.K. Matsopoulos* and K.S. Nikita*,

*School of Electrical and Computer Engineering National Technical University of Athens Iroon
 Politechniou 9, Zografos 15780, HELLAS

ekarali@biosim.ntua.gr

Abstract: In this paper, different automatic registration schemes based on global and local optimization techniques in conjunction with different similarity measures are compared in terms of accuracy and efficiency. Results from every optimization procedure are quantitatively evaluated with respect to the manual registration, which is the standard registration method used in clinical practice. The comparison has shown automatic registration schemes based on CD consist of an accurate and reliable method that can be used in clinical ophthalmology, as a satisfactory alternative to the manual method

Introduction

Retinal images are the common diagnostic tool in ophthalmology. Many eye diseases, like diabetic retinopathy, glaucoma and age-related macular degeneration can be detected in ophthalmic images, and many therapeutic techniques are implemented according to eye vessels topography, as it is presented in ophthalmic images [1]. Comparison studies of ophthalmic images require thorough visual inspection because of their spatial misalignment. Manual registration is the standard method used in clinical practice, however it depends on human knowledge and experience. On the other hand, many automatic registration schemes that combine speed and accuracy have been applied to retinal images[2][3] [4].

The most common ophthalmic imaging techniques are fluorescein angiography (FA) and indocyanine green angiography (ICG). FA images the fluorescence of a dye, fluorescein, as it travels through retinal vessels because of blood circulation. Soon after intravenous injection to the patient of sodium fluorescein 10% (usually after 5-7sec), FA images are obtained at a rate of 1 image/sec for the next 20sec. Prior to any examination, a Red-Free (RF) image is acquired using a green filter, which cuts off the red light. In RF images, retinal blood vessels appear dark. Information from RF images in combination with FA and/or ICG data is used for the evaluation of disease progress [1].

In this work, automatic registration schemes based on intrinsic image characteristics are compared in terms of accuracy and efficiency. In particular, two transformation models, namely affine and projective transformation, three standard similarity measures, namely cross-correlation coefficient (C_{cc}), mutual

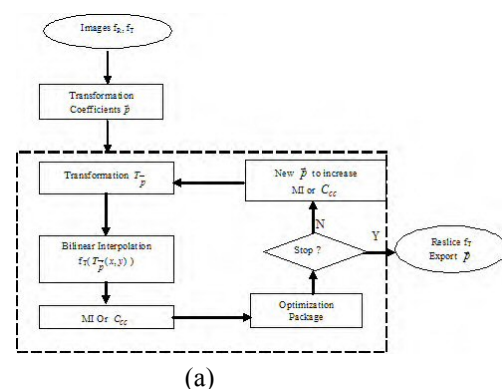
information coefficient (MI) and chamfer distance (CD) have been used in combination with four different common optimization algorithms: Downhill Simplex (DSM), Powell's Method (PM), their combination (DSM-PM) and a combination of Simulated Annealing (SA) with PM (SA-PM). Results from every optimization procedure have been quantitatively evaluated with respect to the manual registration

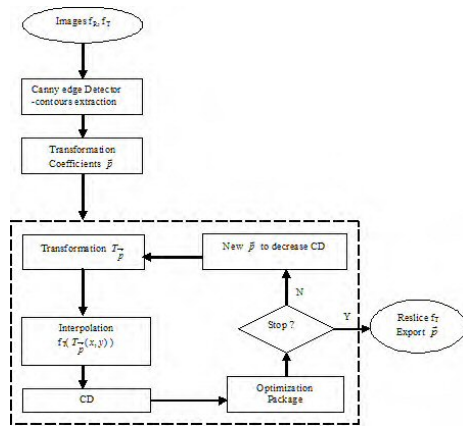
Materials and Methods

Image Acquisition: Retinal images were obtained using the IMAGENet 1024 system. A CCD camera mounted on the Topcon TRX-50X, a fundus camera that provides 50% of coverage, 39mm working distance and special filters for FA, acquired digital ophthalmic images of size 1024x1024 pixels. All registration techniques were applied to retinal images of size 512x512 to increase optimization algorithm convergence speed.

Registration schemes: An automatic registration technique is determined by the chosen transformation model, the similarity metric and the optimization strategy. In this work (a) intensity and (b) segmentation based registration schemes have been implemented (Fig.1). The intensity based registration schemes use C_{cc} or MI as similarity function while the segmentation based technique use CD as similarity measure between registered contour images.

No preprocessing step was required for registration schemes based on C_{cc} or MI. Optimization techniques based on minimization of CD were applied to edge images of the retina, which were derived from the corresponding gray level images by applying first a canny edge detector with standard deviation $\sigma = 3$ and then the reconstruction opening operator that links edge fragments.





(b)

Figure 1.a) Flowchart of intensity and b) segmentation based registration methods, where f_R is the reference image and f_T is the image to be transformed, T_p is in general the transformation model and \vec{p} is the vector of transformation parameters.

Transformation model:

Affine transformation: A 2D affine transformation [2] maps every pixel (x, y) of an image I to a pixel (x', y') of a reference image J according to the equation:

$$\begin{pmatrix} x' \\ y' \end{pmatrix} = \begin{pmatrix} a_1 & a_2 \\ a_3 & a_4 \end{pmatrix} \begin{pmatrix} x \\ y \end{pmatrix} + \begin{pmatrix} d_x \\ d_y \end{pmatrix} \quad (1)$$

Projective Transformation: A 2D projective transformation [4] maps every pixel (x, y) of an image I to a pixel (x', y') of a reference image J according to the equation:

$$\begin{pmatrix} wx' \\ wy' \\ w \end{pmatrix} = \begin{pmatrix} a_1 & a_2 & a_3 \\ a_4 & a_5 & a_6 \\ a_7 & a_8 & 1 \end{pmatrix} \begin{pmatrix} x \\ y \\ 1 \end{pmatrix} \quad (2)$$

Similarity measures:

Cross-correlation coefficient (C_{cc}) is a statistical similarity measure, suitable for registering monomodal medical images [2]. The C_{cc} between two images I and J of size $M \times N$ pixels is mathematically expressed by:

$$C_{cc} = \frac{\sum_{x=1}^M \sum_{y=1}^N (I(x, y) - \bar{I})(J(x, y) - \bar{J})}{\sqrt{\sum_{x=1}^M \sum_{y=1}^N (I(x, y) - \bar{I})^2 \sum_{x=1}^M \sum_{y=1}^N (J(x, y) - \bar{J})^2}} \quad (3)$$

where \bar{I} and \bar{J} are the mean gray values of I and J respectively and $C_{cc} \in [-1, 1]$. Registration with C_{cc} is successful only when the gray levels of the two images are linearly associated

Mutual Information (MI) can be considered as a generalized non-linear correlation function. Considering two images I and J , which are geometrically associated by a transformation T , if a and b are the gray values of $I(x, y)$ and $J(T(x, y))$ respectively, then the coefficient of MI, $MI(I, J)$ can be mathematically expressed by:

$$MI(I, J) = \sum_{a, b} p_{IJ}(a, b) \ln \frac{p_{IJ}(a, b)}{p_I(a)p_J(b)} \quad (4)$$

where $p_{IJ}(a, b)$ corresponds to the joint probability distribution of I and J and $p_I(a)$ and $p_J(b)$ are the marginal probabilities distributions of gray values a of image I and b of image J , respectively. A disadvantage of MI is that it usually presents many local extremes in which the optimization procedure may be trapped, which reduces registration efficiency and reliability. Furthermore MI based registration schemes are sensitive to the used interpolation method [5].

Chamfer Distance (CD): Two binary contour images are precisely aligned when the mean CD between them is minimum. 2D CD is computed by applying a suitable mask [6]. Usually the referenced contour distance map is computed prior to registration and used as a look-up table during the optimization procedure. CD minimization is independent of the images gray level variances. However registration based on CD is efficient when the image that contains the most contour information is assumed as the reference image.

Optimization methods:

Downhill Simplex method (DSM), due to Nelder and Mead [7], is mostly recommended on applications that require execution speed over accuracy. In this work, DSM was implemented as presented in [7]. The termination criterion was set equal to 10^{-6} .

Powell's direction set method (PM) finds the minimum of the similarity function in the N -dimensional parameter space, by iteratively minimizing the function in one direction along the set of N conjugate different directions. PM is considered a thorough registration technique; however it may be trapped to a local minimum of the function. PM was implemented as described in [7]. The initial set of directions was considered to be the basis vector in each dimension. The termination criterion were determined as in DSM implementation.

Simulated Annealing method (SA) is commonly used in registration applications to extract similarity function's global minimum hidden among many local minima [7]. The concept of the method relies on thermodynamics' laws and depends on the mathematical expression of the similarity function, the generation function of the random steps, the acceptance criterion and the annealing schedule. In this paper the VFSA has been implemented but with the same annealing schedule for all the transformation parameters, namely $T = T_0 e^{-0.22k}$, where $T_0 = 0.1$ and $k_{max} = 100$. Due to the stochastic nature of SA algorithm, the Powell's algorithm was sequentially employed in order to provide more stable outputs.

Results

In this work the registration schemes were assessed on 23 retinal image pairs, 18 temporal RF pairs and 5 FA-RF pairs. The temporal RF images were taken up to five years apart. The optimization techniques, DSM,

PM, DSM-PM and SA-PM were combined with each of the two transformation models, affine and projective and with each of the three similarity measures; C_{cc} , MI and CD. PM was implemented after DSM or SA. For the registration methods based on affine transformation the search space was restricted, so that $a_1, a_4 \in [-1.01, 1.01]$, $a_2, a_3 \in [-0.1, 0.1]$, and $dx, dy \in [-150, 150]$ pixels. For the registration schemes based on projective transformation the search space was restricted, so that $a_1, a_5 \in [-1.01, 1.01]$, $a_2, a_4 \in [-0.1, 0.1]$, $a_3, a_6 \in [-150, 150]$ pixels and $a_7, a_8 \in [10^{-4}, 10^{-6}]$. Bilinear interpolation was used and checkerboard images of the registration were produced to allow visual assessment of every method. As reference image was taken the one that had more edge information.

The registration schemes were compared to the manual method, which was performed by an expert. From every image pair, six pairs of bifurcation points were chosen, according to which the affine transformation parameters were calculated using the Least-Squares method (LSM). This procedure was repeated three times. The best set of parameters was chosen as the one that corresponded to the smallest associated Root Mean Square Error (RMSE) value. The average RMSE of the LSM was 0.77 pixels, a very low value that shows the good accuracy during pair points definition.

One thousand edge points of the image-to-be-transformed from each pair were randomly chosen. They were transformed according to the manual and the automatic extracted transformation model. The mean RMSE between the manual and automatic registered points was computed. In Fig.2 the mean RMSE of the different registration schemes are presented. The obtained errors of the automatic techniques were calculated according to the equation: $RMSE = \sqrt{RMSE_{manual}^2 + RMSE_{automatic}^2}$ (4)

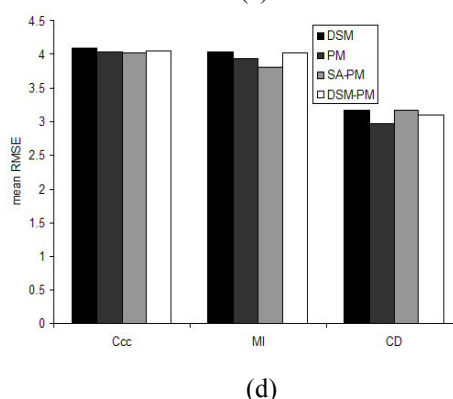
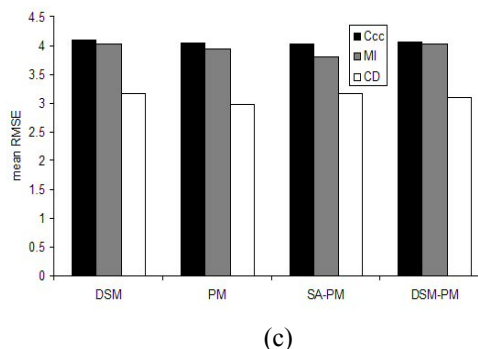
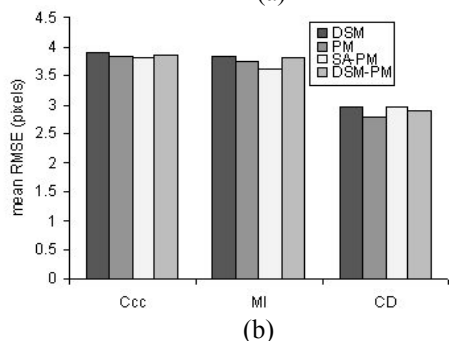
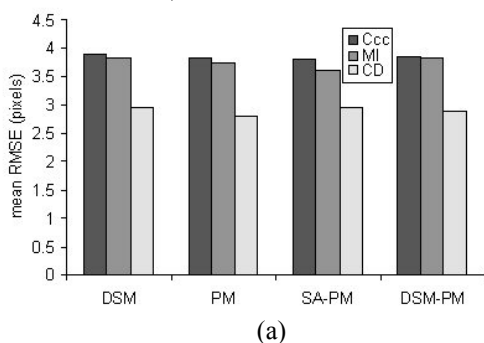


Figure 2. (a) Mean RMSE of C_{cc} , MI and CD for DSM, PM, SA-PM, DSM-PM based on affine transformation. (b) Mean RMSE of DSM, PM, SA-PM, DSM-PM for C_{cc} , MI and CD based on affine transformation. (c) Mean RMSE of C_{cc} , MI and CD for DSM, PM, SA-PM, DSM-PM based on projective transformation. (d) Mean RMSE of DSM, PM, SA-PM, DSM-PM for C_{cc} , MI and CD based on projective transformation

Discussion

According to Fig.2 all optimization algorithms present the same registration accuracy. Moreover, DSM is the fastest method (average time 29.9 s) and needs the lowest number of iterations (on average 396). PM seems to be very slow (119.9 s) because of the small steps it takes in the parameter space. DSM-PM presents an average performance of DSM and PM, as far as execution time (79.9s) and number of iterations (962) are concerned. Almost all optimization techniques depend on the shape of the similarity measure. If it has many extremes, then the optimization algorithms must be initialized close to the best solution. Only SA, which represents a global optimization technique, is almost independent from the initial guess of the values of the transformation parameters.

C_{cc} did not succeed in registering FA-RF image pairs, due to the nonlinear dependence between the gray levels of the images. Also C_{cc} , according to Fig.2 (b) and (d) presents high registration errors in comparison with CD. MI shows almost the same registration accuracy with C_{cc} . MI coefficient is well coupled with SA-PM, which does not present a strong dependence on the initial solution. CD is the most accurate similarity measure and represents an excellent approximation of the manual method. CD does not depend on the gray levels of the images and according to Fig.2 (b) and (d)

can be combined well with all optimization techniques, when contour extraction from images is possible.

According to Fig. 2 registration schemes based on affine transformations represents smaller registration errors that registration methods based on projective transformation. Spatial misalignment among retinal images of the same patient is usually due to large horizontal displacements because of changes in patient position in temporal images, and due to smaller vertical displacements caused by chin cup movements. Small angle rotations are due to different head bow or eye movement. Differences in scaling are caused by changes in distance between patient's head and the camera. Affine model takes into account these factors of translation, scaling and rotation.

Fig.6 shows three different retinal image pairs, registered with different schemes. As can be seen from the images there is absolute continuity between vessels, something that shows the success of the registration scheme.

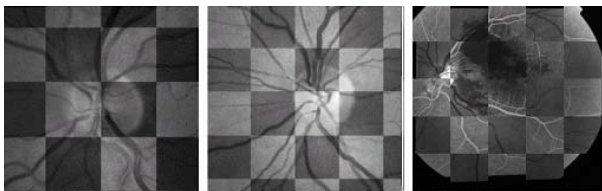


Figure 3. (a) Chessboard image of a temporal RF image pair registered by PM combined with C_{cc} . (b) chessboard image of a temporal RF image pair registered by SA-PM coupled with MI. (c) chessboard image of an FA-RF image pair registered with DSM-PM combined with CD. All these registration schemes are based on the affine transformation.

Conclusions

In this work different automatic registration schemes were applied to temporal RF retinal images and to FA-

RF retinal image pairs, and were evaluated according to the manual registration. The comparison showed that registration schemes based on CD approximate the best the standard manual technique, and can be used in clinical practice as a robust and faster alternative to the manual method.

References

- [1] SAINE P. AND TYLER M., (2002): *Ophthalmic Photography: Retinal Photography, Angiography and Electronic Imaging*. 2nd ed. Butterworth-Heinemann Medical; 2002.
- [2] RITTER, N. et al, (1999): 'Registration of Stereo and Temporal Images of the Retina', *IEEE Trans. on Medical Imaging*, vol. 18, pp. 404-418, 1999.
- [3] LALIBERTE, F.; GAGNON, L. (2003): 'Registration and Fusion of Retinal Images-An Evaluation Study', *IEEE Trans. on Medical Imaging*, vol. 22, pp. 661-673, 2003.
- [4] MATSOPOULOS, G. ; MOURAVLIANSKY, N. ; DELIBASIS, K.; NIKITA, K.S. (1999): 'Automatic Retinal Image Registration Scheme Using Global Optimization Techniques', *IEEE Trans. on Inf. Tech. in Biomedicine*, vol 3, pp. 47-60, 1999.
- [5] PLUIM, J. et al, (2003): 'Mutual information based registration of medical images: a survey', *IEEE Trans. on Medical Imaging*, vol. 22, pp. 986-1004, 2003.
- [6] BORGEFORS, G. (1984): 'Distance Transformations in Arbitrary Dimensions', *Com. Vision Graphics and Image Processing* vol. 27, pp. 321-345, 1984.
- [7] PRESS, W.H.; FLANNERY, B.P.; TEUKOLSKY, S.A.; VETTERLING, W.T. (1992): 'Numerical Recipes in C: The Art of Scientific Computing', Cambridge University Press 1992.